0026-895X/11/7906-941–952$25.00
MOLECULAR PHARMACOLOGY
Vol. 79, No. 6
69534/3691107
Mol Pharmacol 79:941–952, 2011
Printed in U.S.A.

Phosphatase and Tensin Homolog Deleted on Chromosome 10 (PTEN) Inhibition by 4-Hydroxynonenal Leads to Increased Akt Activation in Hepatocytes[S]

Colin T. Shearn, Rebecca L. Smathers, Benjamin J. Stewart, Kristofer S. Fritz, James J. Galligan, Numsen Hail, Jr., and Dennis R. Petersen

Departments of Pharmaceutical Sciences (C.T.S., K.S.F., N.H., D.R.P.), Toxicology (R.L.S.), and Pharmacology (J.J.G.), School of Pharmacy (C.T.S., R.L.S., K.S.F., N.H., D.R.P.), and School of Medicine (J.J.G.), University of Colorado Denver, Aurora, Colorado; and Center for Accelerator Mass Spectrometry, Lawrence Livermore National Laboratory, Livermore, California (B.J.S.)

Received October 25, 2010; accepted March 17, 2011

ABSTRACT

The production of reactive aldehydes such as 4-hydroxynonenal (4-HNE) is proposed to be an important factor in the etiology of alcoholic liver disease. To understand the effects of 4-HNE on homeostatic signaling pathways in hepatocytes, cellular models consisting of the human hepatocellular carcinoma cell line (HepG2) and primary rat hepatocytes were evaluated. Treatment of both HepG2 cells and primary hepatocytes with subcytotoxic concentrations of 4-HNE resulted in the activation of Akt within 30 min as demonstrated by increased phosphorylation of residues Ser473 and Thr308. Quantification and subsequent immunocytochemistry of phosphatidylinositol-3,4,5-trisphosphate [PtdIns(3,4,5)P_3[rsqb$_1$ resulted in a 6-fold increase in total PtdIns(3,4,5)P_3 and increased immunostaining at the plasma membrane after 4-HNE treatment. Cotreatment of HepG2 cells with 4-HNE and the phosphatidylinositol 3-kinase (PI3K) inhibitor 2-(4-morpholinyl)-8-phenyl-4*H*-1-benzopyran-4-one (Ly294002) or the protein phosphatase 2A (PP2A) inhibitor okadaic acid revealed that the mechanism of activation of Akt is PI3K-dependent and PP2A-independent. Using biotin hydrazide detection, it was established that the incubation of HepG2 cells with 4-HNE resulted in increased carbonylation of the lipid phosphatase known as "phosphatase and tensin homolog deleted on chromosome 10" (PTEN), a key regulator of Akt activation. Activity assays both in HepG2 cells and recombinant PTEN revealed a decrease in PTEN lipid phosphatase activity after 4-HNE application. Mass spectral analysis of 4-HNE-treated recombinant PTEN detected a single 4-HNE adduct. Subsequent analysis of Akt dependent physiological consequences of 4-HNE in HepG2 cells revealed significant increases in the accumulation of neutral lipids. These results provide a potential mechanism of Akt activation and cellular consequences of 4-HNE in hepatocytes.

Introduction

Oxidative modification of proteins by reactive aldehydes has been implicated in an increasing number of hepatic disease states, including hepatitis C, nonalcoholic steatohepatitis, and chronic alcoholic liver disease (Paradis et al., 1997; Seki et al., 2002; Roede et al., 2008). A documented marker for increased oxidative stress in cells is the presence of elevated levels of 4-hydroxynonenal (4-HNE). Reactive aldehydes such as 4-HNE originate from peroxidation of membrane lipids, including linoleic acid (Poli et al., 2008). 4-HNE is a potent electrophile that will react with nucleophilic functional groups in DNA as well as Cys, Lys, and His residues within proteins. Proteins documented to be targets for modification by 4-HNE include protein disulfide isomerase, actin,

This work was supported by the National Institutes of Health Institutes of Alcohol Abuse and Alcoholism [Grants R37-AA009300-14, 1-F32-AA018613-01A1, 1-F31-AA018898-01].

Article, publication date, and citation information can be found at http://molpharm.aspetjournals.org.

doi:10.1124/mol.110.069534.

[S] The online version of this article (available at http://molpharm.aspetjournals.org) contains supplemental material.

ABBREVIATIONS: 4-HNE, 4-hydroxynonenal; PTEN, phosphatase and tensin homolog deleted on chromosome 10; PH, Pleckstrin homology; PtdIns(3,4,5)P_3, phosphatidylinositol-3,4,5-trisphosphate; ROS, reactive oxygen species; rPTEN, recombinant PTEN; LB, Luria broth; DTT, dithiothreitol; Ly294002, 2-(4-morpholinyl)-8-phenyl-4*H*-1-benzopyran-4-onePAGE; TBST, Tris-buffered saline with 1% Tween 20; DCFDA, 2′,7′-dichlorofluorescein diacetate; DCF, dichlorofluorescein; TR-FRET, time-resolved fluorescence resonance energy transfer; PBS, phosphate-buffered saline; DTT, dithiothreitol; DiC_8, dioctanoyl; MALDI-TOF, matrix-assisted laser desorption ionization/time of flight; TBS, Tris-buffered saline; GFP, green fluorescent protein; eGFP, enhanced green fluorescent protein; PtdIns(3,4)P_2, phosphatidylinositol-3,4-bisphosphate; TAPP1, phosphatidylinositol binding protein tandem-PH-domain-containing protein-1; OA, okadaic acid; PAGE, polyacrylamide gel electrophoresis; PHLPP, pleckstrin homology domain leucine-rich repeat protein phosphatases; PI3K, phosphatidylinositol 3-kinase; PP2A, protein phosphatase 2A.

and thioredoxin (Carbone et al., 2005; Ozeki et al., 2005; Fang and Holmgren, 2006). Consistent with the potent electrophilic properties of 4-HNE, proteins modified by this biogenic aldehyde displayed compromised function.

Hepatocytes are well recognized for their ability to withstand oxidative stress associated with the production 4-HNE (Esterbauer et al., 1991). Previous studies have shown that hepatocytes metabolize 4-HNE to its glutathione conjugate, which is then rapidly exported out of the cell. Treatment of rat H35 hepatoma cells with 25 μM 4-HNE resulted in approximately 61% of the 4-HNE being converted to the glutathione adduct and exported out of the cells within 2 to 5 min (Tjalkens et al., 1999). In HepG2 cells, 4-HNE exposure at concentrations as high as 100 μM for 2 h did not induce cell damage or death, as indicated by changes in DNA or by lactate dehydrogenase release (Stewart et al., 2009). In other studies using primary hepatocytes, 500 μM 4-HNE was metabolized to the metabolites 4-hydroxynonenoic acid and 1,4-dihydroxynonene within 2 min (Hartley and Petersen, 1997).

The oncoprotein Akt is involved in the activation of cell survival pathways after oxidative insult. For example, in cells exposed to 1 mM hydrogen peroxide, Akt is phosphorylated on Thr308 and Ser473, leading to its complete activation and resulting in increased cell survival. Under conditions of increased oxidative stress, Akt activation involves the oxidation and subsequent inactivation of PTEN (phosphatase and tensin homolog deleted on chromosome 10) (Leslie et al., 2003). As an initial step, Akt is recruited to the membrane by the association of its Pleckstrin homology (PH) domain with phosphatidylinositol-3,4,5-trisphosphate [PtdIns(3,4,5)P_3]. Once at the membrane, Akt is phosphorylated on Thr308 by phosphoinositide-dependent kinase 1 (PDK1), followed by phosphorylation at Ser473 by mTORC2 (for comprehensive review, see Liao and Hung, 2010).

The primary regulator of Akt is the tumor suppressor PTEN. PTEN negatively regulates AKT activation via its lipid phosphatase activity (Di Cristofano and Pandolfi, 2000). PTEN is a phosphatidylinositol 3-phosphatase catalyzing the removal of the 3-position phosphate from PtdIns(3,4,5)P_3 to produce phosphatidylinositol-4,5-bisphosphate. PTEN is also susceptible to oxidative stress. Both ROS and reactive nitrogen species have been shown to modify and inactivate PTEN (Lee et al., 2002; Yu et al., 2005). Inactivation of PTEN leads to increased Akt activation in both cellular and animal models. In addition, hepatocyte-specific deletion of PTEN leads to steatohepatitis and increased hepatocellular carcinoma in mice (Horie et al., 2004). Initiation of liver steatosis in these mice was linked with increased Akt activation and subsequent Akt-dependent downstream activation of sterol regulatory element-binding protein-1c, peroxisome proliferator-activated receptor γ, and Forkhead box, class O1 (Watanabe et al., 2005).

In this communication, we describe the effects of 4-HNE on activation of Akt in a hepatocellular cell line as well as primary hepatocytes. Our results demonstrate that PTEN activity is inhibited after exposure to 4-HNE, resulting in increased Akt activation as determined by increased Akt phosphorylation. Furthermore, we demonstrate that the inhibition of PTEN coincides with adduction by 4-HNE. This report provides insight into the mechanisms of 4-HNE induced cellular signaling with respect to fatty acid production and liver injury induced by oxidative stress.

Materials and Methods

Preparation of Recombinant PTEN. Full-length recombinant PTEN (rPTEN) was amplified by polymerase chain reaction from pGEX4T-PTEN using the following oligonucleotides: PTEN-5′ (5′-CCACATGACAGCCATCATCAAAGAG-3′ sense) and PTEN-3′ (5′-TCAGACTTTTGTAATTTGTGAATGCTG-3′ antisense). After amplification, each fragment was TOPO-cloned into His-tagged pET100-TOPO (Invitrogen, Carlsbad, CA), transformed into TOP-10 cells, and grown overnight on LB-ampicillin plates (100 μg/ml) according to the manufacturer's instructions. Colonies were picked and placed into 3-ml LB cultures for 16 h with 100 μg/ml ampicillin. DNA was subsequently purified using QIAGEN Minipreps (QIAGEN, Valencia, CA), and sequences were verified at the University of Colorado Cancer Center core facility. All oligonucleotides were purchased from Integrated DNA Technologies, Inc. (Coralville, IA).

To express the histidine-tagged rPTEN, rPTEN-pET100 DNA was transformed into BL-21 Star (DE3) *Escherichia coli*, and colonies were picked and grown in 3 ml of LB plus 100 μg/ml ampicillin. After 16 h, 1 ml of the culture was added to 100 ml of fresh LB together with ampicillin, and the culture was grown until it reached an OD_{600} of 0.8 to 1.0. The culture was then induced with 1 mM isopropyl-β-D-thiogalactopyranoside and grown for 4 h at 37°C. Cultures were sedimented by centrifugation at 6000 rpm for 20 min and flash-frozen. For protein purification, pellets were thawed and cells were lysed on ice for 20 min in 50 mM HEPES, pH 7.6, 300 mM NaCl, 10 mM imidazole, 2 mM DTT, 0.5% Triton X-100, together with lysozyme and protease inhibitors (Sigma). This sample was sonicated with three 20-s bursts, followed by centrifugation at 14,000 rpm for 30 min. The supernatant was decanted, 150 μl of 50% immobilized nickel resin (QIAGEN) in lysis buffer was added, and the sample was incubated for 4 h at 4°C on a rotary mixer. After incubation, the beads were washed five times with 50 mM HEPES, pH 7.6, and 300 mM NaCl containing 20 mM imidazole and 2 mM DTT, then twice increasing to 50 mM imidazole, and finally eluted from the resin with 50 mM HEPES, pH 7.6, 300 mM NaCl, 150 mM imidazole, 10% glycerol, and 2 mM DTT.

Cell Culture. HepG2 cells were maintained at 50 to 80% confluence in RPMI 1640 medium supplemented with 10% fetal bovine serum, 100 mM HEPES, 100 IU/ml penicillin, and 100 g/ml streptomycin. Before each experiment, cells were plated into six-well plates at a density of 10^6 cells per well in RPMI 1640 medium plus serum and allowed to adhere overnight. The following day, the cells were washed twice in serum-free RPMI 1640 medium and treated with indicated doses of 4-HNE in serum-free medium. Where indicated, Ly294002 (50 μM preincubation/60 min) or okadaic acid (0.1 μM preincubation/30 min) (Calbiochem/EMD, Gibbstown, NJ) were added with RPMI 1640 medium plus serum and also in the serum-free medium used for each 4-HNE treatment.

Western Blotting. Cells were lysed for 5 min in 50 mM HEPES, 100 mM NaCl, 1% Triton X-100, 2 mM EDTA, pH 7.7, plus protease inhibitors (Sigma-Aldrich, St. Louis, MO), followed by sonication for 3×10 s and 20 μg loaded per well on 7% SDS-PAGE gels, electroblotted to polyvinylidene difluoride, blocked in Tris-buffered saline with 1% Tween 20 (TBST) and 5% nonfat dry milk for 1 h, and incubated overnight in primary antibody. The following rabbit polyclonal primary antibodies were used at 1:1000 dilution in TBST: pSer473 Akt, p-Thr308 AKT, total Akt, p-PTEN and total PTEN (Cell Signaling Technology, Danvers, MA). The rabbit polyclonal 4-HNE antibody was used at 1:1000 as described previously (Stewart et al., 2007). The following morning blots were washed three times for 5 min each in TBST and incubated for 1 h in horseradish peroxidase-conjugated goat polyclonal anti-rabbit secondary antibody (Jackson ImmunoResearch laboratories, West Grove, PA). Blots were washed three times for 5 min each in TBST and subsequently developed using chemiluminescence (Pierce SuperSignal; Thermo Fisher Scientific, Waltham, MA) and developed on film.

Isolation of Rat Primary Hepatocytes. All animal procedures were approved by the Institutional Animal Care and Use Committee at the University of Colorado Denver Anschutz Medical Campus. Primary rat hepatocytes were isolated from the livers of untreated, laboratory chow-fed male Sprague-Dawley rats (~400 g) that were purchased from The Jackson Laboratory (Bar Harbor, ME). The isolation procedure used a modified collagenase perfusion method. Hepatocytes were resuspended in RPMI 1640 medium containing 10% fetal bovine serum, and penicillin/streptomycin (100 IU/ml and 100 g/ml, respectively). Cell viability was assessed using Trypan blue exclusion, with viability exceeding 90%. Cells (10^6) were plated in six-well plates coated with extracellular matrix gel from Engelbreth-Holm-Swarm murine sarcoma (Sigma-Aldrich), and allowed to acclimate to culture conditions at 37°C + 5% CO_2 for 2 h before treatments.

Determination of ROS Production. To determine the production of ROS within the cell, a fluorescent indicator was used, [2′,7′-dichlorofluorescein diacetate (DCFDA)]. Cells in six-well plates were washed twice in Krebs-Ringer buffer solution followed by the addition of 20 μM DCFDA and increasing concentrations of 4-HNE in Krebs-Ringer buffer in triplicate wells for each treatment. The plates were then read at the dichlorofluorescein (DCF) emission wavelength of 538 nm using a SpectraMax Gemini EM dual-scanning microplate spectrofluorometer (Molecular Devices, Sunnyvale, CA). A time-course reading was evaluated every 5 min throughout a 120-min period. As a control, DCFDA and 4-HNE were also incubated in the absence of cells, and no fluorescence was detected.

TR-FRET quantification of PtdIns(3,4,5)P_3 in HepG2 cells. Cells (10^6) were plated, allowed to adhere overnight, and treated with either serum-free medium (control) or 100 μM 4-HNE in serum-free RPMI 1640 medium for 60 min. Cells were washed twice in PBS, and PtdIns(3,4,5)P_3 was extracted as described in the PtdIns(3,4,5)P_3 Quantification HTRF Assay kit (Millipore, Billerica, MA). After extraction, extracted PtdIns(3,4,5)P_3 was placed in a 96-well microtiter plate, and the displacement of biotinylated PtdIns(3,4,5)P_3 from a complex consisting of europium-labeled anti-glutathione transferase antibodies, a glutathione transferase-tagged PH domain, biotinylated PtdIns(3,4,5)P_3, and streptavidin-allophycocyanin. The displacement of the biotinylated PtdIns(3,4,5)P_3 by extracted cellular PtdIns(3,4,5)P_3 resulted in a decrease in the fluorescent emission of europium complex after excitation at 330 nm and emission at 620 nm and 665 nm. All plates were read on a Synergy H4 Hybrid Multi-Mode Microplate reader (BioTek Instruments, Winooski, VT). Concentrations of PtdIns(3,4,5)P_3 were obtained by plotting the ratio of E_{665}/E_{620} multiplied by 10,000 using Prism 4 software (GraphPad Software, San Diego, CA) according to the manufacturer's instructions.

Adduction of Recombinant PTEN by 4-HNE. Two micrograms of rPTEN was treated with 4-HNE at molar ratios of 1:1 and 10:1 for 30 min at 37°C. Samples were then boiled in 5× SDS loading buffer, run on a 7.5% SDS-PAGE gel, and Western-blotted using anti-4-HNE polyclonal antibodies. To verify PTEN adduction, membranes were then stripped for 15 min using stripping buffer (Thermo Fisher Scientific), washed twice in TBST, and blocked once again for 1 h in TBST 5% nonfat dry milk. After blocking, membranes were incubated overnight with mouse anti-PTEN (Cell Signaling Technology) and subsequently processed.

Biotin Hydrazide Modification of Carbonylated PTEN. To determine reactive aldehyde adduction, 10^7 HepG2 cells were treated with 100 μM 4-HNE for 1 h in serum-free medium. Cells were then lysed in 50 mM HEPES, 100 mM NaCl, 2 mM EDTA, and 2.5 mM biotin hydrazide and allowed to incubate for 30 min at room temperature. To remove excess biotin, lysates were dialyzed overnight at 4°C. Biotinylated proteins were purified by incubating with streptavidin agarose beads (Thermo Fisher) on a rotary mixer at 4°C

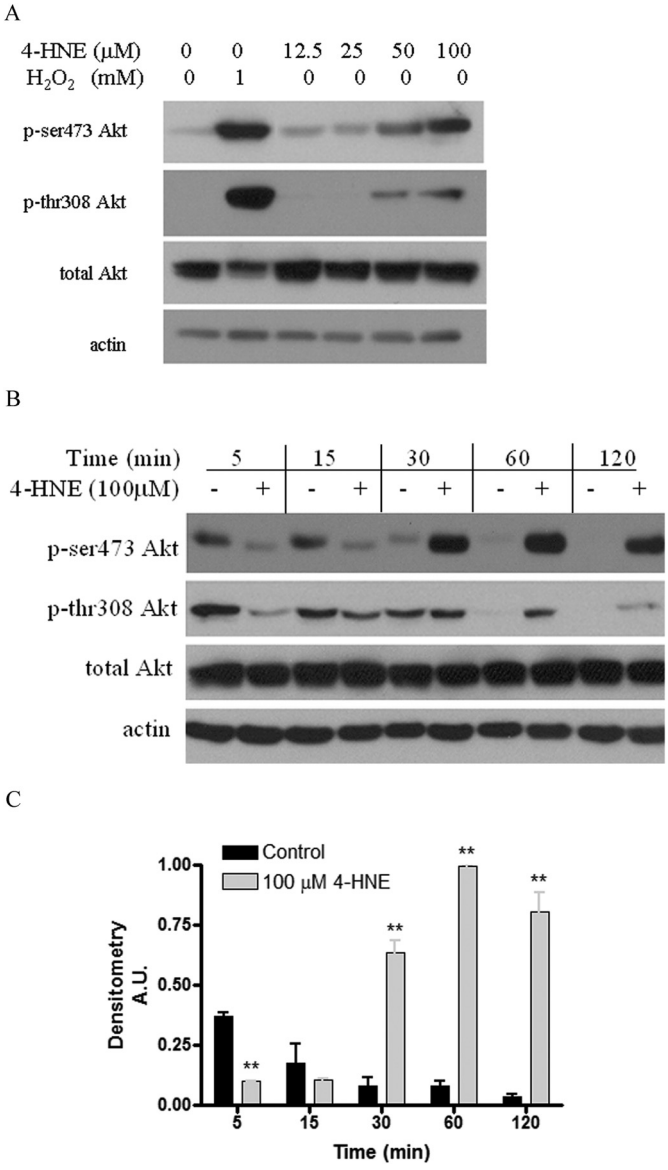

Fig. 1. Time course and dose dependence of 4-HNE-induced Akt phosphorylation. HepG2 cells were washed twice in serum-free media and treated with increasing concentrations of 4-HNE in serum-free media for 1 h (A) or 100 μM 4-HNE from 5 to 120 min in serum-free media (B). Cells were lysed, run on an 8% SDS PAGE, blotted, and probed for p-Ser473 Akt, p-Thr308Akt, total Akt and actin. C, densitometric analysis of p-Ser473Akt/Akt/Actin. Blots are representative of at least three independent experiments. **, $p < 0.001$. A.U., arbitrary units.

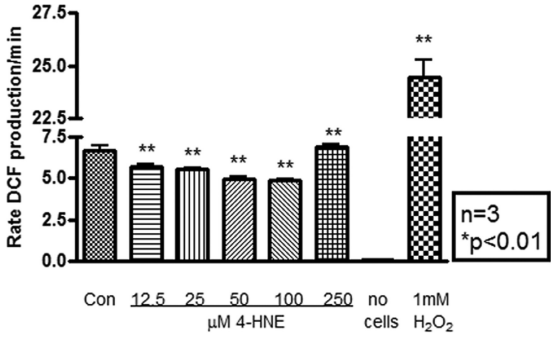

Fig. 2. Fluorescence measurements of intracellular ROS generation after 4-HNE addition. Relative rate of ROS generation (DCF production per minute) after the addition of increasing concentrations of 4-HNE in serum-free media for 2 h. HepG2 cells were incubated in triplicate with increasing concentrations of 4-HNE (0–250 μM) or 1 mM H_2O_2 in the presence of 10 μg/ml 2′,7′-dichlorofluorescein diacetate at 37°C. **, $p < 0.01$.

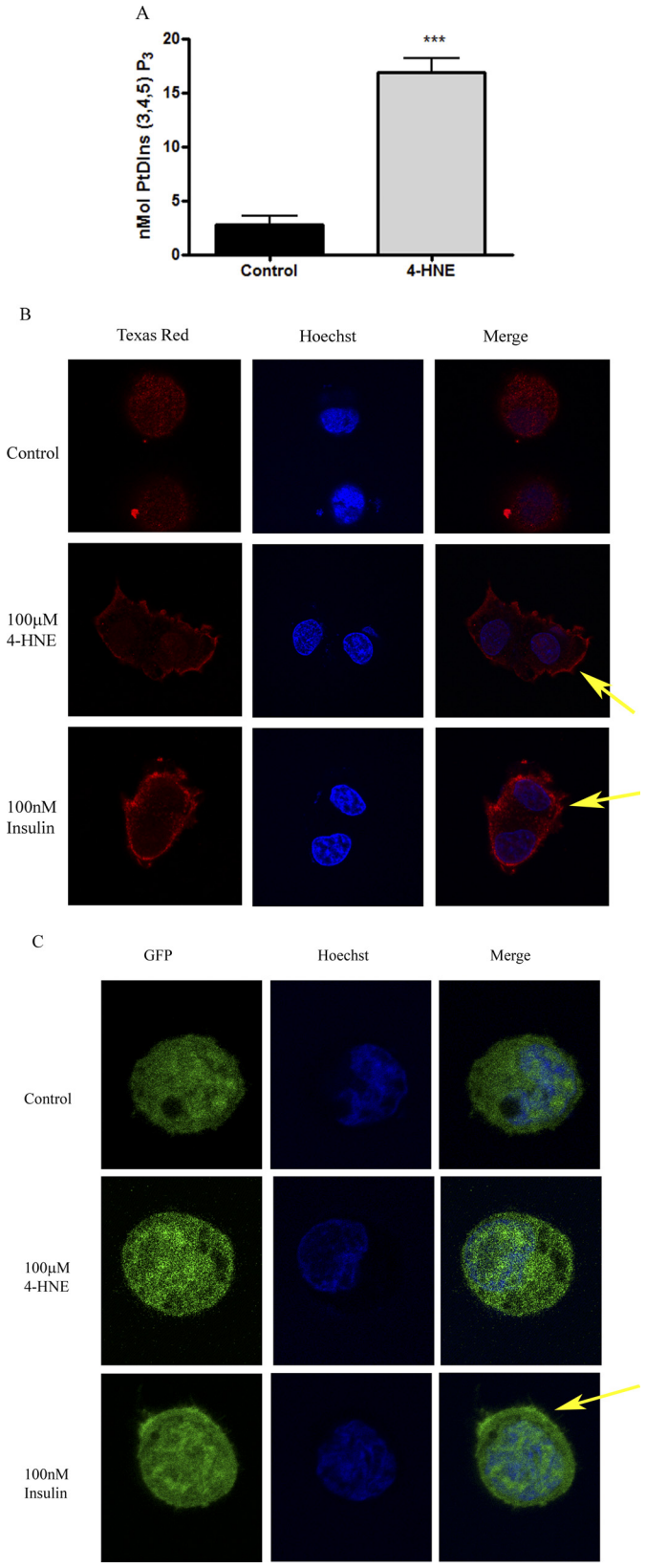

Fig. 3. Characterization of 4-HNE-mediated PtdIns(3,4,5)P_3 production in HepG2 cells. A, quantification of PtdIns(3,4,5)P_3 by using TR-FRET. Cells were treated with or without 100 μM 4-HNE (60 min) in serum-free media. Cells were lysed and PtdIns(3,4,5)P_3 was extracted and quantified as described under *Materials and Methods*. All samples were performed in triplicate. ***, $p < 0.001$. B, cells were treated with or without 100 μM 4-HNE (60 min) or 100 nM insulin (15 min). The cells then underwent immunofluorescence staining with mouse-monoclonal anti-PtdIns(3,4,5)P_3 and an anti-mouse secondary antibody conjugated to Texas Red [red, PtdIns(3,4,5)P_3; blue, Hoechst 33342 nuclear staining]. C, confocal microcopy of eGFP-TAPP1 transfected HepG2 cells stimulated with 100 μM 4-HNE (60 min) and 100 nM insulin (15 min) (green, eGFP-TAPP1; blue, Hoechst 33342 nuclear staining; yellow arrows indicate increased plasma membrane staining).

for 3 h, washed five times in PBS, loaded onto SDS-PAGE gels, and processed according to Western blotting protocols.

In Vitro PTEN Activity Assay. To assess activity of recombinant untreated and 4-HNE-treated PTEN, a phosphate release assay was used with BIOMOL Green (Enzo Life Sciences, Inc., Farmingdale, NY) as an indicator. For each assay, 2 μg of rPTEN was incubated for 30 min at room temperature with increasing molar amounts of 4-HNE in 50 mM tricine and 100 mM NaCl, pH 8.0. Unreacted 4-HNE was quenched using 2 mM DTT for 30 min at room temperature. Phosphatase assays were performed in 50 μl of reaction buffer, 200 μM water-soluble DiC_8-PtdIns(3,4,5)P_3 (Echelon, Salt Lake City, UT) for 40 min at 37°C. The reactions were stopped, and the released phosphate was measured by incubating the samples for 20 min with 200 μl of BIOMOL Green. After incubation, samples were read using a microtiter plate reader at 620 nm on a SpectraMax 190 microplate spectrofluorometer (Molecular Devices). Values were determined as nanomoles of PtdIns(3,4,5)P_3 released per min and subsequently converted to percentage of control reactions.

MS Analysis of 4-HNE-Modified Recombinant PTEN. 4-HNE-exposed human rPTEN (Cayman Chemical, Ann Arbor, MI) was examined to determine whether protein adduction occurred in vitro. In brief, 2.4 μg (0.05 nmol) of rPTEN was incubated with a 5× molar excess of 4-HNE (0.25 nmol) for 30 min at 25°C. The control and treated samples were concentrated using C18 ZipTips (Millipore, Billerica, MA), mixed 1:1 with sinapinic acid (10 mg/ml) and spotted in 1-μl aliquots onto an Opti-TOF 96-well insert (Applied Biosystems, Foster City, CA). An ABI 4800 Plus MALDI-TOF mass spectrometer (Applied Biosystems) was used to characterize the adduction of rPTEN by 4-HNE. The instrument was operated under standard conditions for intact protein at a laser power of 5500 and was calibrated using the 1+ and 2+ charge states of bovine serum albumin. MS analysis was performed using standard linear high mass acquisition and processing methods with a focus mass of 50 kDa. Data analysis was performed by using 4000 Series Explorer ver. 3.5 (Applied Biosystems).

Cellular PTEN Activity Assay. After treatment, HepG2 cells were lysed in 50 mM HEPES, 100 mM NaCl, 1% Triton X-100, and 2 mM EDTA plus protease inhibitors. Lysates were subsequently precleared with protein A agarose beads (Sigma-Aldrich) for 1 h. To the cleared lysates, fresh protein A agarose and 2 μg of rabbit polyclonal anti-PTEN was added, and the samples were incubated on a rotomixer overnight at 4°C. Samples were washed four times in lysis buffer, and activity assays were performed according to in vitro protocol except that incubation with substrate was for 30 min on a rotary mixer. Beads were separated by centrifugation at 1000*g*, and supernatants were placed in 96-well microtiter plates. Phosphate release was measured using BIOMOL Green as described under *In Vitro PTEN Activity Assay*.

Nile Red Staining and Confocal Microscopy. HepG2 cells were grown on glass coverslips and treated with 4-HNE or colchicine for 1 h and allowed to recover for 24 h. Cells were fixed with 10% neutral buffered formalin for 30 min at room temperature, and the coverslips were then extracted for 20 min at room temperature with PBS, pH 7.4, containing 2.5% bovine serum albumin and 1% Triton X-100. Cover slips were then washed three times for 5 min each with TBS. For Nile red neutral lipid staining, after fixation, extraction, and washing, coverslips were incubated with 20 μg/ml Nile red in TBS for 30 min and washed once in TBS and mounted with 4,6-diamidino-2-phenylindole-containing mounting medium (Vector Laboratories, Burlingame, CA). Confocal images were taken with a

100× oil immersion objective on a Nikon Eclipse TE2000-E instrument (Nikon, Melville, NY), with identical instrument laser and contrast settings used within each group. Images were acquired using Nikon EZ-C1 software.

Nile Red Cellular Neutral Lipid Accumulation Assay and Cellular DNA Measurement. HepG2 cells were grown on six-well plates to greater than 90% confluence and were treated for 1 h with 4-HNE, Brefeldin A, diethyl maleate, oleic acid conjugated to BSA, or colchicine, followed by a 24-h recovery in serum-containing RPMI 1640 medium. Nile red was used to detect cellular neutral lipid using a modification of previously reported techniques, and Hoechst 33342 was used to measure cellular DNA (McMillian et al., 2001). Cells were collected in 1 ml of phenol red-free, serum-free RPMI 1640 medium, and 50 μl of cell suspension was incubated in sterile 96-well fluorescence plates for 1 h at 37°C with 200 μl of serum-free, phenol red-free RPMI 1640 medium containing Nile red at 20 μg/ml and Hoechst 33342 at 10 μg/ml. Plates were shaken for 10 s before reading, and neutral lipid was assessed by Nile red fluorescence with excitation at 485 nm and emission at 565 nm and was normalized against cellular DNA as measured by Hoechst 33342 staining measured with excitation at 355 nm and emission at 465 nm.

Immunocytochemical Analysis of PtdIns(3,4,5)P_3 in HepG2 cells using Confocal Microscopy. HepG2 cells (2×10^5) were plated on coverslips in six-well plates for 24 h in RPMI 1640 medium + 10% serum. The following morning, cells were washed two times in serum-free RPMI 1640 medium and treated with 100 μM 4-HNE (60 min) or 100 nM insulin (30 min). After treatment, cells were washed once in PBS and fixed in 3.7% paraformaldehyde in PBS for 30 min. After fixation, cells were washed once in PBS and permeabilized using 0.15% Triton X-100 in PBS for 10 min. Cells were then incubated for 1 h in RPMI 1640 medium plus 10% bovine serum (blocking reagent), washed twice in PBS, and incubated overnight in mouse monoclonal anti-PtdIns(3,4,5)P_3 (Echelon Biosciences, Salt Lake City, UT) with RPMI 1640 medium and 2% bovine serum. Plates were washed three times for 10 min each in PBS followed by incubation for 60 min in Texas red-conjugated goat anti-mouse secondary antibody (Invitrogen). Coverslips were washed twice in PBS, mounted using Vectastain mounting medium (Vector Laboratories) with 10 μg/ml Hoechst 33342/Supermount [1:4; from Sigma and Biogenex (San Ramon, CA), respectively] and allowed to dry at 4°C overnight. Slides were then analyzed using confocal microscopy, Texas red fluorescence (excitation at 485 nm/emission at 565 nm) Hoechst 33342 staining (excitation at 355 nm/emission at 465 nm).

Confocal Microscopy of GFP-TAPP1 Localization in HepG2 Cells. HepG2 cells (2×10^7) were electroporated with 30 μg of GFP-phosphatidylinositol binding protein tandem-PH-domain-containing protein-1 (TAPP1; kind gift from Dr. A. J. Marshall, University of Manitoba, Winnipeg, MB, Canada) or eGFP control in 200 μl of PBS (without Ca^{2+}or Mg^{+}) using a Gene Pulser at 960 μF, 300 V, 29 μs (Bio-Rad Laboratories, Hercules, CA). Cells (2×10^5) were subsequently plated into six-well plates containing coverslips and allowed to adhere overnight. Cells were washed twice in serum-free RPMI 1640 medium and treated with 100 μM 4-HNE (60 min) or 100 nM insulin (30 min). After treatment, cells were washed twice in PBS and mounted using Vectastain mounting medium with 10 μg/ml Hoechst 33342 and allowed to dry at 4°C overnight. Slides were then analyzed using confocal microscopy-GFP (excitation at 395 nm/emission at 488 nm) Hoechst 33342 staining (excitation at 355 nm/emission at 465 nm).

Statistical Analysis. Relative densitometry of Western blots was quantified using ImageJ (http://rsb.info.nih.gov/ij/). All data and statistical analysis was performed using one-way analysis of variance and Prism 4 for Windows (GraphPad Software, San Diego, CA). All data are expressed as mean ± S.E. and p values <0.05 were considered significant.

Results

4-HNE Activates Akt via a Concentration-Dependent Mechanism. The PTEN/Akt pathway has been implicated in increased cell survival after cellular stress (Lee et al., 2002; Yu et al., 2005). Full activation of Akt requires sequential

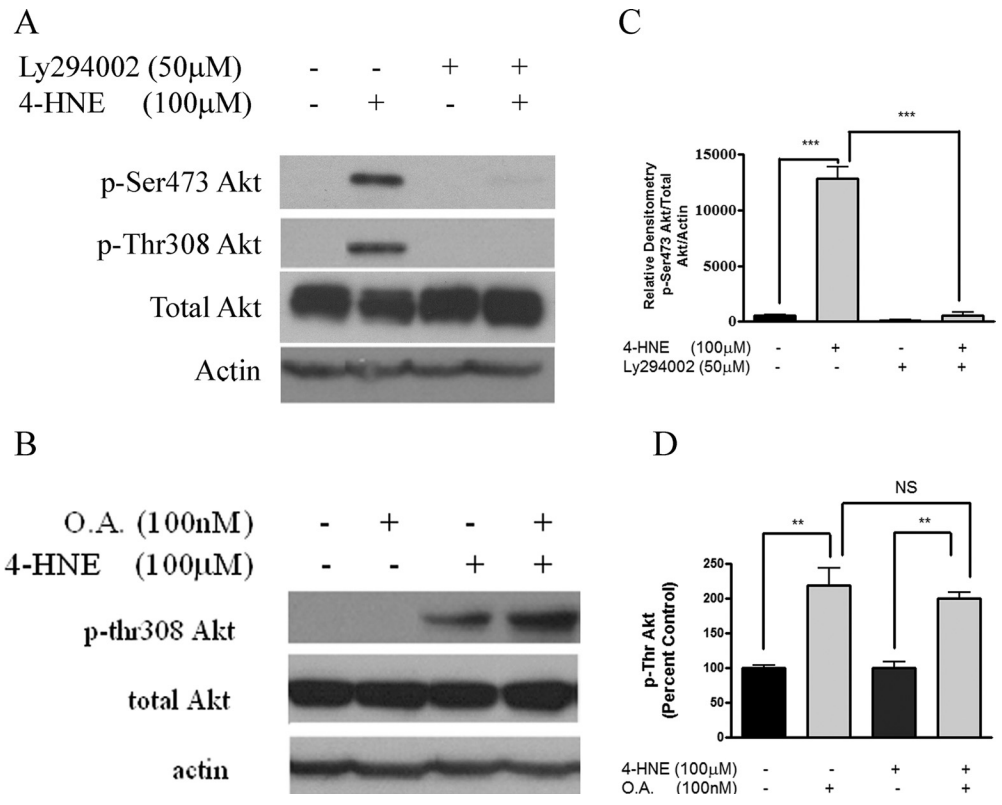

Fig. 4. Effect of Ly294002 and okadaic acid on 4-HNE-induced Akt phosphorylation. A, increased phosphorylation of Akt is PI3K-dependent but not PP2A-dependent. Cells were treated in serum-free media with 100 μM 4-HNE or control for 60 min after preincubation with Ly294002 (50 μM, 60 min) (A) or okadaic acid (O.A.; 100 nM, 30 min) (B). After treatment, cells were lysed and Western blotted for phosphorylation of Akt on Ser473 (Ly294002) or Thr308 (okadaic acid). C, densitometric analysis of p-Thr308Akt/total Akt/Actin from Western blots presented in B. D, densitometric analysis of the blots presented in B. Okadaic acid (O.A.) samples represented as percentage control (absence of okadaic acid compared with presence of okadaic acid). Western blots were quantified using ImageJ and analyzed using one-way-analysis of variance and Prism software. **, $p < 0.01$; ***, $p < 0.001$.

phosphorylation on both Thr308 and Ser473 (Liao and Hung, 2010). To evaluate the effect of 4-HNE on Akt in HepG2 cells, cells were exposed to increasing concentrations of 4-HNE (0–100 μM) for 60 min in serum-free medium (Fig. 1A). As a positive control, 1 mM H_2O_2 (5 min) was added. Cells were subsequently lysed and Western blots probed for increased levels of phosphorylation on Ser473 and Thr308 of Akt. It is apparent from Fig. 1A that Akt is not phosphorylated in control samples, whereas both Ser473 and Thr308 are phosphorylated at concentrations of 4-HNE ranging from 25 to 100 μM.

To further explore the time course of Akt activation, a time course (0–120 min) was performed using 100 μM 4-HNE in serum-free medium (Fig. 1B). As expected, in the untreated controls, removal of serum for 2 h showed a progressive decrease in Akt phosphorylation in the control. 4-HNE, however, led to an initial decrease in Akt phosphorylation within 5 min followed by an increase in phosphorylation by the 30-min time point extending to 120 min. Densitometric analysis indicated that Akt phosphorylation at Ser473 peaks at 60 min with a statistically significant decrease by 120 min (Fig. 1C). Overall, these data demonstrate a concentration- and time-dependent activation of Akt after 4-HNE treatment.

ROS is a known regulator of Akt activation, and 4-HNE has been linked to increased ROS production in certain cell types (Raza and John, 2006; Go et al., 2007). To dissociate ROS-mediated Akt activation from 4-HNE, cells were treated with increasing doses of 4-HNE in serum-free medium and examined for the oxidation of 2′,7′ dichlorofluorescin to DCF over a 120-min period. From Fig. 2, incubation of HepG2 cells with concentrations of 4-HNE below 250 μM led to a decrease in the rate of ROS generation as detected via the oxidation of DCFDA compared with untreated cells. As a positive control for this assay, 1 mM hydrogen peroxide led to a dramatic short-term increase in DCF production that was suggestive of enhanced ROS production. To establish that lack of ROS production was dependent on the time of exposure to 4-HNE, ROS was measured over a 2-h period in serum-free medium. Similar rates of ROS production occurred throughout the time course (Data not shown). These data suggest an ROS-independent mechanism of Akt activation by 4-HNE.

Effects of 4-HNE on PtdIns(3,4,5)P_3 and PtdIns(3,4)P_2 in HepG2 cells. Previous biochemical studies have shown that stimulation of Akt activation requires production of PtdIns(3,4,5)P_3 or PtdIns(3,4)P_2 (Liao and Hung, 2010). To examine the effects of 4-HNE on overall concentrations of PtdIns(3,4,5)P_3, time-resolved fluorescence resonance energy transfer (TR-FRET) was used. The data presented in Fig. 3A demonstrate a 6-fold increase in cellular PtdIns(3,4,5)P_3 concentrations after 4-HNE treatment. To further characterize changes in intracellular PtdIns(3,4,5)P_3, confocal microscopy and immunocytochemistry were performed using anti-PtdIns(3,4,5)P_3 antibodies. In Fig. 3B, compared with control cells, increased PtdIns(3,4,5)P_3 staining is evident at the plasma membrane (arrows) in both the 4-HNE-treated and insulin-treated cells.

TAPP1 binds specifically to PtdIns(3,4)P_2 and has been shown to be regulated by insulin (Marshall et al., 2002; Wullschleger et al., 2011). To gain a better understanding of the intracellular effects of 4-HNE on PtdIns(3,4)P_2, GFP-tagged TAPP1 domain (Fig. 3C) or eGFP (Supplemental Fig. 1) alone was overexpressed in HepG2 cells. After 24 h, cells were stimulated with either 4-HNE (100 μM, 60 min) or insulin (100 nM, 30 min) in serum-free medium and examined using confocal microscopy. As shown in Supplemental Fig. 1, neither 4-HNE nor insulin had any effect on localization of eGFP. In Fig. 3C, GFP-TAPP1 localization is primarily cytosolic in unstimulated cells. We were surprised to find that 4-HNE did not have an effect on TAPP1 localization; insulin, however, showed a mild increase in plasma mem-

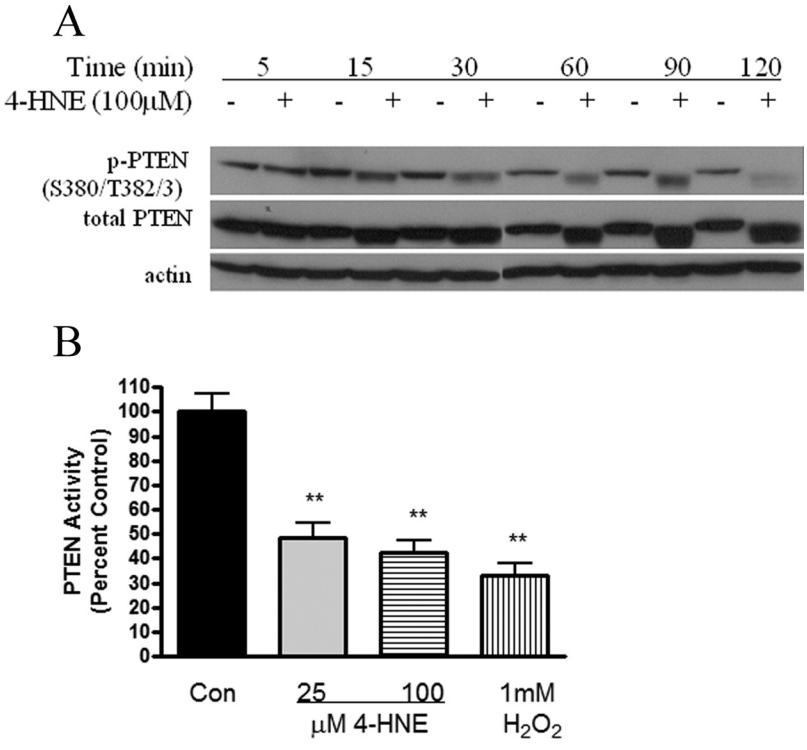

Fig. 5. Effects of 4-HNE on PTEN phosphorylation and activity. A, phosphorylation state of PTEN. Cells were treated in serum-free media with 100 μM 4-HNE or without (control) for 0 to 2 h. After treatment, cells were lysed, and 20 μg of protein was loaded onto a 7% SDS PAGE gel as described under *Materials and Methods*. B, PTEN activity is inhibited by 4-HNE in HepG2 cells. Cells were treated in serum-free media with 25,100 μM 4-HNE for 60 min or 1 mM H_2O_2 for 10 min and lysed, and then PTEN activity was measured using a malachite green phosphate release assay and DiC_8 PtdIns(3,4,5)P_3. All samples were performed in triplicate. **, $p < 0.01$. Con, control.

brane accumulation of GFP-TAPP1 (arrows). Combined, these data suggest that 4-HNE treatment leads to an increase in PtdIns(3,4,5)P_3 production but not an increase in PtdIns(3,4)P_2 production.

Activation of Akt by 4-HNE is PtdIns(3,4,5)P_3-Dependent. Full activation of Akt requires phosphorylation of Thr308 and Ser473. To further understand the mechanism of Akt activation after 4-HNE treatment, HepG2 cells were incubated with either a PI3K inhibitor [inhibitor 2-(4-morpholinyl)-8-phenyl-4*H*-1-benzopyran-4-one (Ly294002; Fig. 4A)] or a protein phosphatase 2A inhibitor (PP2A) [okadaic acid (OA)] (Fig. 4B, short exposure; Supplemental Fig. 2, long exposure). It is evident from Fig. 4A that Akt activation was significantly reduced after preincubation of Ly294002. Quantification and statistical analysis of Fig. 4A indicate a statistically significant (95%) reduction in Ser473 phosphorylation after Ly294002 incubation (Fig. 4C). These data suggest a PI3K-dependent mechanism of Akt activation by 4-HNE. In Fig. 4B, preincubation with okadaic acid increased phosphorylation of Thr308 in both the control cells and the 4-HNE-treated cells. Although no change in phosphorylation of Thr308 is evident in the control lanes in Fig. 4B, a longer exposure using the same samples clearly indicates an increase in phosphorylation in the control plus OA samples (Supplemental Fig. 2). Figure 4D represents the quantification of the Western blots in Fig. 4B and Supplemental Fig. 2. A comparison of the control samples and the 4-HNE-treated samples indicated a similar 2-fold change in both the control/control OA and the 4-HNE/4-HNE OA samples.

The dephosphorylation of Akt on Ser473 has been determined to not be a substrate of PP2A but is a substrate of PHLPP. Therefore, okadaic acid should have no effect on Ser473 phosphorylation (Liao and Hung, 2010). There was no change in phosphorylation on Ser473 after OA treatment of 4-HNE-treated cells (Supplemental Fig. 3A). Although no inhibitors of PHLPP are available, total levels were examined by Western blot, and no significant changes in protein expression were seen (Supplemental Fig. 3B). As mentioned previously, Akt is phosphorylated at Thr308 by PDK1, which is thought to be a constitutively active enzyme that also is recruited to the membrane by a PtdIns(3,4,5)P_3-dependent mechanism (Bayascas, 2008). 4-HNE had no effect on phosphorylation of PDK1 or total levels of PDK1 in HepG2 cells (Supplemental Fig. 3B). Collectively, these data suggest that Akt activation occurs via a PI3K-dependent mechanism and is not dependent on the inactivation of Akt-specific protein phosphatases.

PTEN Phosphorylation Is Decreased after 4-HNE Exposure. In cells, PTEN serves as a negative regulator of Akt by dephosphorylating the PI3K product PtdIns(3,4,5)P_3. Regulation of PTEN occurs via phosphorylation of C-terminal residues Ser380/Thr382/383, leading to an inactive state (Vazquez et al., 2001). To determine whether 4-HNE affected the phosphorylation state of the C terminus of PTEN, HepG2 cells were exposed to 100 μM 4-HNE for a time course of 5 to 120 min (Fig. 5A). We were surprised to find that a time-dependent dephosphorylation occurs on the C terminus of PTEN after 4-HNE treatment. The change in phosphorylation is also associated with an increase in the overall migration of PTEN (Fig. 5A). To further explore the phospho-status of PTEN, HepG2 cells were pretreated with okadaic acid and lysed, and the phospho-status of PTEN was examined. No change in PTEN phosphorylation was evident after PP2A inhibition (data not shown).

In cells, C-terminal dephosphorylation activates PTEN, leading to decreased Akt activation (Vazquez et al., 2001). This is contrary to what is actually observed in our model. To determine the effects of 4-HNE on PTEN activity in HepG2 cells, PTEN activity assays were performed using immunoprecipitated PTEN from 4-HNE-treated HepG2 cells. As a positive control, 1 mM hydrogen peroxide was used to verify PTEN inhibition (Lee et al., 2002; Leslie et al., 2003). As shown in Fig. 5B, at the 25 μM 4-HNE concentration, PTEN activity decreased 50% compared with control, suggesting that although PTEN is dephosphorylated, activity is inhibited by 4-HNE. Thus, the decrease in overall PTEN activity, in addition to the decrease in PTEN phosphorylation, suggests an alternative mechanism of regulation of this phosphatase.

PTEN Is Carbonylated after 4-HNE Treatment in HepG2 Cells. To determine whether cellular PTEN is adducted by 4-HNE, a method of biotin hydrazide modification of protein-bound reactive aldehydes was employed (Fig. 6A) (Grimsrud et al., 2007). HepG2 cells were exposed to 100 μM 4-HNE, treated with 2.5 mM biotin hydrazide, and purified using streptavidin beads. Western blot analysis of streptavidin pull-down assays indicates an increase in PTEN carbony-

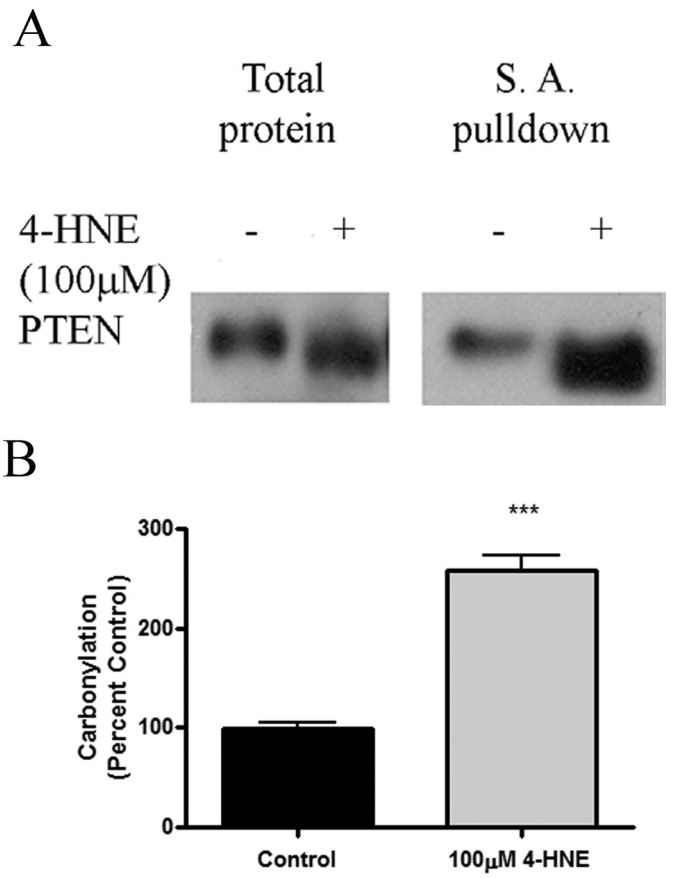

Fig. 6. Biotin hydrazide modification and examination of PTEN in 4-HNE-treated HepG2 cells. A, streptavidin pull-down assay of 4-HNE-modified PTEN from HepG2 cells. Protein (125 μg) from 4-HNE-treated (100 μM/60 min in serum-free media) or untreated cells was incubated for 2 h with 2.5 mM biotin hydrazide and purified using a streptavidin pull-down assay. Samples were subsequently analyzed using SDS PAGE/Western blotting with rabbit polyclonal anti-PTEN. All samples were performed in triplicate. B, densitometric analysis of Western blots. ***, $p < 0.001$.

lation (reactive aldehyde modification) after 4-HNE exposure. Subsequent quantification of the Western blots demonstrates a 2.5-fold increase in aldehyde-modified PTEN in 4-HNE-treated cells compared with controls (Fig. 6B). Overall, these data demonstrate intracellular carbonylation of PTEN readily occurs as a consequence of exposure to physiologically relevant concentrations of 4-HNE.

Characterization of PTEN Modification by 4-HNE In Vitro. To further examine the effects of 4-HNE on PTEN activity, recombinant PTEN (rPTEN) was treated with increasing molar ratios of 4-HNE followed by Western blotting using 4-HNE-specific polyclonal antibodies and PTEN PtdIns(3,4,5)P_3 activity assays. The data presented in Fig. 7A demonstrate that rPTEN is modified by 4-HNE at a concentration of 0.25 μM, which is equivalent to a molar ratio of 1:1. The data in Fig. 7B demonstrate that PTEN is susceptible to inactivation by 4-HNE with an estimated IC_{50} of 1.5 μM. This value corresponds to a molar ratio of approximately 2.5 to 5 mol of 4-HNE per mole of rPTEN, consistent with the cellular data demonstrating PTEN modification and inhibition by 4-HNE (Fig. 6). To further substantiate the ability of 4-HNE to modify PTEN, MALDI-TOF mass spectrometry was performed. The MALDI-TOF mass spectrometry data presented in Fig. 8 confirm modification of PTEN by 4-HNE. After 4-HNE modification at a molar ratio of 5:1, a mass shift of 156Da was detected corresponding to the Michael-addition of 1 mol of 4-HNE to rPTEN.

Effects of 4-HNE on Lipid Accumulation. Previous reports have suggested a link between increased hepatic oxidative stress and lipid accumulation (Grattagliano et al., 2008; Sorrentino et al., 2010). We therefore sought to characterize the effects of reactive aldehydes generated as a result of oxidative stress on cellular neutral lipid accumulation by HepG2 cells. After a 1-h exposure to 100 μM 4-HNE and a 24-h recovery period, a significant increase ($p < 0.01$) in cellular neutral lipid was observed (Fig. 9A). Confocal microscopy experiments, using Nile red staining of cellular lipids, confirmed an increase as a result of 4-HNE treatment, whereas colchicine treatments were not discernibly different from control cells (Fig. 9B). Because microtubule disruption (colchicine) and Golgi complex disruption (Brefeldin A) impair export of lipids from hepatocytes, cellular lipid accumulation was measured after treatment with these compounds as well as with the glutathione-depleting agent diethyl maleate (Fig. 9C). These treatments failed to alter cellular neutral lipid content, whereas oleic acid conjugated to bovine serum albumin dramatically increased cellular lipid accumulation. Taken together, these results demonstrate 4-HNE-dependent increases in lipid accumulation in HepG2 cells.

Akt Is Activated by 4-HNE in Primary Hepatocytes. All of the previous experiments were performed in the HepG2 hepatocellular carcinoma cell line. To verify that Akt is also activated after 4-HNE treatment in primary cells, primary rat hepatocytes were isolated and plated on Matrigel (BD Biosciences, San Jose, CA), and experiments were performed using increasing concentrations of 4-HNE (0–100 μM). The dose-response experiments presented in Fig. 10A demon-

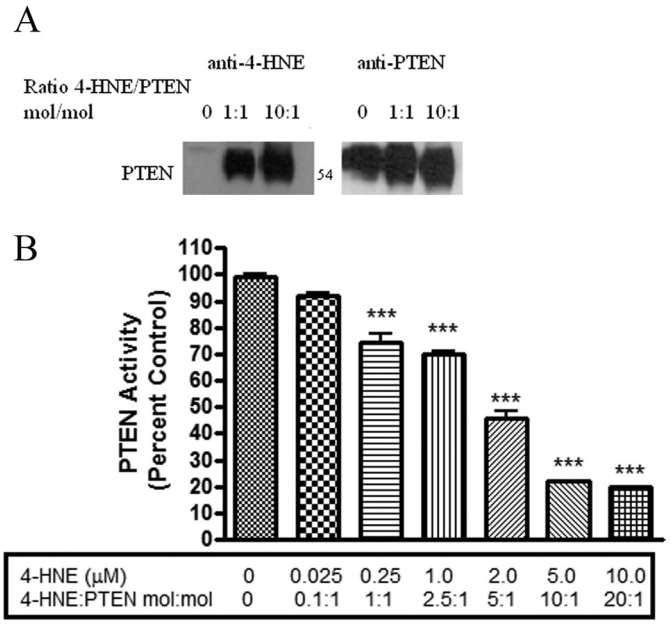

Fig. 7. Effects of 4-HNE on recombinant PTEN. A, Western blotting of rPTEN treated with increasing molar ratios of 4-HNE. Purified PTEN was incubated with increasing molar ratios of 4-HNE for 30 min at room temperature. Samples were boiled in 5× SDS loading buffer, run on an 8% SDS PAGE gel, blotted, and probed for 4-HNE using anti-4-HNE polyclonal antibodies. Blots were stripped and reprobed for PTEN. B, inhibition of rPTEN by 4-HNE treatment. Purified rPTEN was incubated with increasing molar ratios of 4-HNE and phosphate release activity assays performed using PtdIns(3,4,5)P_3 DiC_8 as a substrate as described under *Materials and Methods*. The data presented were derived from three independent experiments. Statistical analysis was via one-way analysis of variance. *, $p < 0.05$; **, $p < 0.01$.

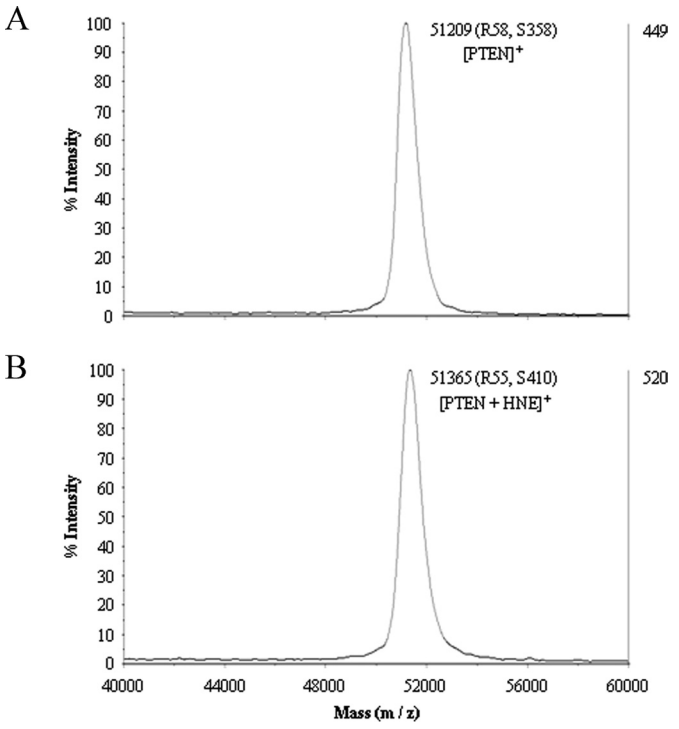

Fig. 8. MS analysis of unmodified and 4-HNE-modified rPTEN. The mass spectra obtained for control (A) and 4-HNE treated rPTEN (B) details a mass shift of 156 Da in the treated intact protein, corresponding with a mass addition of a 4-HNE Michael-type adduct. The unmodified protein displays an isotopic mass average of 51,209 *m/z*, with a resolution of 58 and a signal-to-noise ratio of 358. The 4-HNE-modified protein has an observed *m/z* of 51,365 kDa, with a resolution of 55 and a signal-to-noise ratio of 410. Although this mass shift indicates one predominant 4-HNE adduct, given the expected instrument resolution at this mass-to-charge ratio, the presence of native PTEN and PTEN with multiple 4-HNE modifications is likely.

strate that Akt phosphorylation after exposure to 100 μM 4-HNE is consistent with the results presented in Fig. 1A. The data presented in Fig. 10B clearly indicate a statistically significant increase in phosphorylation of Akt on Ser473 after treatment of both 50 μM 4-HNE (2-fold) and 100 μM 4-HNE (4-fold) for 1 h. In agreement with the dose response, data presented in Supplemental Fig. 5 demonstrate that time-dependent 4-HNE-mediated Akt phosphorylation in primary hepatocytes is similar to that observed in HepG2 cells (Fig. 1B). Combined, these data confirm that 4-HNE activates Akt both in HepG2 cells and in primary hepatocytes.

Discussion

Chronic liver diseases affect a large percentage of the population today. These diseases include nonalcoholic steatohepatitis and the pathogenic effects of chronic alcoholism (Seki et al., 2002; Roede et al., 2008). A common factor in many of these diseases is their association with oxidative stress and dysregulation of lipid homeostasis. The widely recognized biomarker of oxidative stress 4-HNE is documented to have a number of bioactivities, including covalent modification of protein and DNA, that contribute to increased rates of mutation and altered protein function (Poli et al., 2008). Therefore, understanding the interaction of 4-HNE with cellular pathways and their subsequent mechanisms of activation/inactivation is essential to understanding the pathogenesis of chronic diseases associated with oxidative stress. In this report, we characterize the mechanisms of Akt modulation by 4-HNE HepG2 cells and primary hepatocytes.

Previous studies have demonstrated the ability of ROS to activate Akt via PTEN oxidation (Lee et al., 2002; Leslie et al., 2003). In U87MG cells, 1 mM H_2O_2 resulted in increased

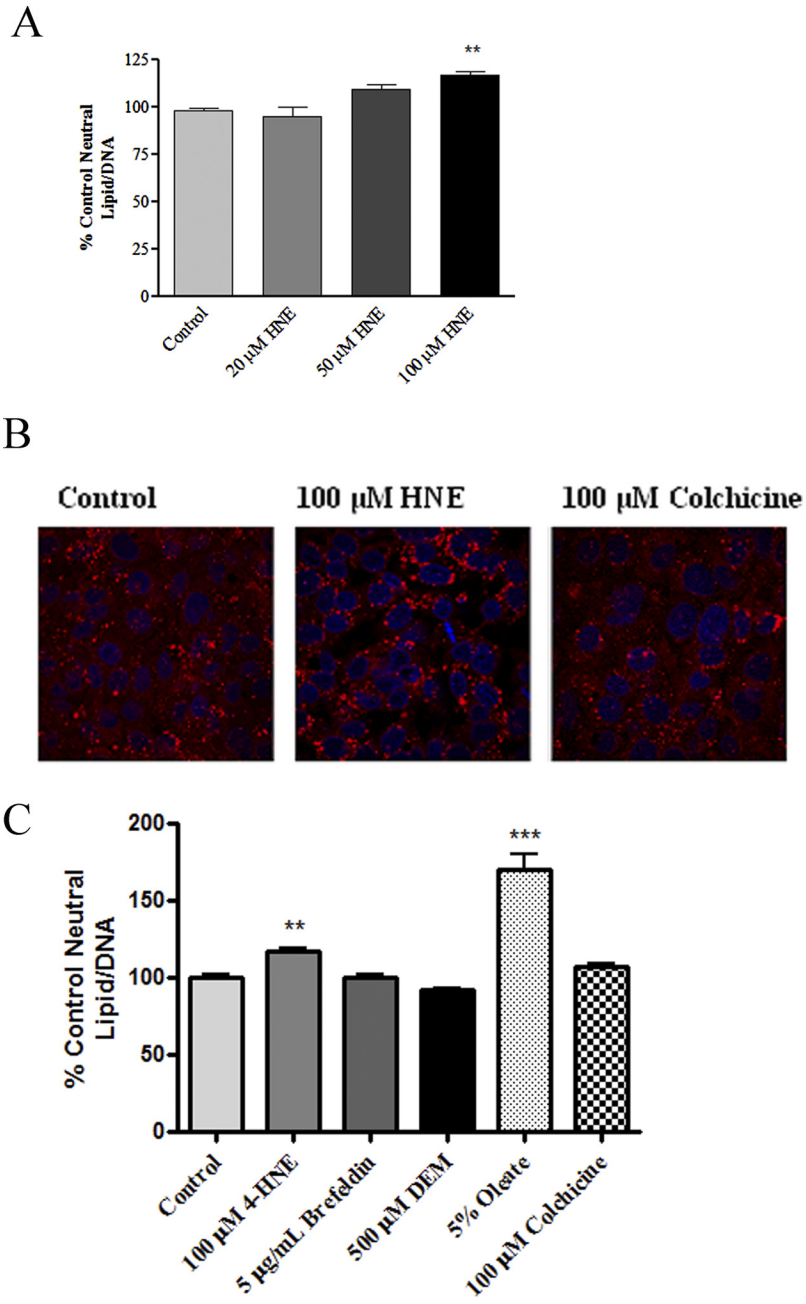

Fig. 9. Effect of 4-HNE addition on lipid accumulation in HepG2 cells. A, 4-HNE neutral lipid effects at 1 h of treatment followed by 24-h recovery. B, Nile red staining for lipid with 1-h treatment and 24-h recovery. Blue, 4,6-diamidino-2-phenylindole nuclear staining; red, Nile red lipid staining. C, neutral lipid effects of 4-HNE, specific pathway disruptors, or oleate. **, $p < 0.01$; ***, $p < 0.001$. DEM, diethyl maleate.

PtdIns(3,4,5)P_3 levels as a result of oxidation and inactivation of PTEN. PTEN-null cells did not exhibit the same increase (Leslie et al., 2003). 4-HNE has been shown to lead to increased production of intracellular ROS in aortic endothelial cells as determined by dichlorofluorescein fluorescence (Go et al., 2007). In Fig. 2 of the present study, treatment of 4-HNE did not lead to the increased production of ROS in HepG2 cells. The absence of measurable ROS suggests 4-HNE-specific effects of Akt activation.

Hepatocytes have been reported to be more resistant than other cell types to 4-HNE-mediated cellular toxicity. Previous reports have suggested that Akt is either activated or inactivated after treatment with 4-HNE in other cell lines. In Jurkat T cells, Akt is down-regulated after 4-HNE exposure under serum-free conditions (Liu et al., 2003). However, these cells have a deletion of PTEN, leading to constitutively activated Akt, which could lead to discrepancies in Akt signaling after 4-HNE treatment (Shan et al., 2000). In neuroblastoma cells, Akt is phosphorylated and activated in response to 4-HNE, yet these experiments were performed in the presence of serum (Dozza et al., 2004). Growth factors in serum are known to activate Akt, which could lead to undesirable complications such as variation in actual concentration and inadvertent activation via growth factor stimulation.

To determine direct effects of 4-HNE on the activation of Akt, 4-HNE was added in the absence of serum. In primary hepatocytes and in HepG2 cells, we demonstrate that there is a corresponding increase in Akt phosphorylation that is both concentration- and time-dependent, reflecting activation of Akt by 4-HNE (Figs. 1, A–C, and 10, A and B, and Supplemental Fig. 5). It should be noted that higher concentrations were required to induce a significant change in phosphorylation in the primary cells compared with the hepatocellular carcinoma cells. This discrepancy could be due to several possibilities, the first being that primary hepatocytes metabolize 4-HNE more effectively because of increased amounts of 4-HNE-metabolizing enzymes such as alcohol dehydrogenase, which is lacking in HepG2 cells (Hartley et al., 1995).

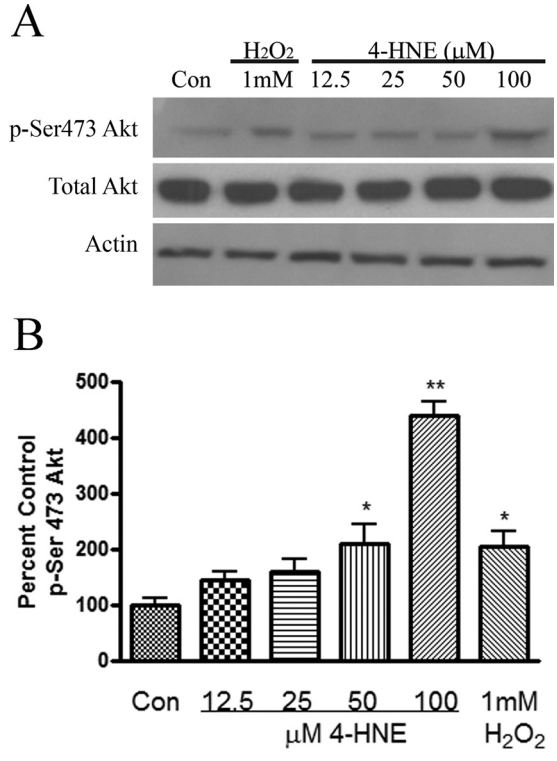

Fig. 10. Dose dependence of 4-HNE on Akt phosphorylation in primary rat hepatocytes. Freshly isolated primary rat hepatocytes were treated with increasing concentrations of 4-HNE (0–100 μM) for 1 h in serum-free media. H_2O_2 (1 mM, 5 min) was used as a positive control for Akt phosphorylation. A, cells were lysed, run on an 8% SDS PAGE, Western blotted, and probed for p-Ser473 Akt, total Akt, and actin. B, quantification of Western blots presented in A. $n = 4$; *, $p < 0.05$; **, $p < 0.01$. Con, control.

As previously mentioned, Akt is regulated by protein phosphorylation/dephosphorylation mechanisms. Protein phosphatases such as PP2A have been shown to be activated by 4-HNE and to dephosphorylate Akt in Jurkat cells, leading to apoptosis (Liu et al., 2003). It is quite possible that PP2A activity is regulated by 4-HNE in hepatocytes. To examine the relative contribution of PP2A, an inhibitor was used. Okadaic acid led to a 2-fold increase in both the control and the 4-HNE-treated cells (Fig. 4B; Supplemental Fig. 2). This indicates that PP2A inhibition does not significantly contribute to the increase in Akt phosphorylation after 4-HNE. To become active, Akt is recruited to the membrane via PtdIns(3,4,5)P_3. The data in Fig. 2, A and B, demonstrate that 4-HNE treatment leads to an increase in PtdIns(3,4,5)P_3 at the plasma membrane. In addition, in Fig. 4A, in the presence of a PI3K inhibitor, 4-HNE inhibited Akt phosphorylation. Combined, these data suggest that 4-HNE-dependent Akt activation is due to increased levels of PtdIns(3,4,5)P_3 and not to PP2A regulation.

By regulating PtdIns(3,4,5)P_3 levels in cells, PTEN is a direct regulator of Akt activation. PTEN is also regulated by phosphorylation. Increased phosphorylation of Ser380 and Thr382/383 in the C terminus of PTEN decreases PTEN stability and activity (Lee et al., 2002; Leslie et al., 2003; Cho et al., 2004; Yu et al., 2005). To determine whether PTEN is regulated by phosphorylation, Western blotting was performed using PTEN phosphospecific antibodies. Based on the observed decrease in PTEN phosphorylation in Fig. 4A, Akt should be not be phosphorylated. However, in this system, Akt is phosphorylated, suggesting that PTEN phosphorylation does not play a role in Akt activation in this system.

PTEN has also been shown to be regulated by direct modification of its active site cysteine. The pK_a of the active site cysteine in PTEN (Cys124) is approximately 4.8, making it a very good nucleophile and target for 4-HNE modification

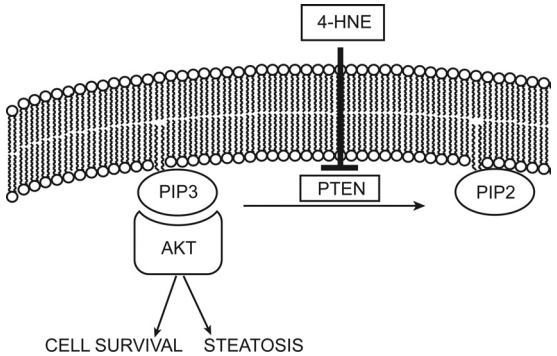

Scheme 1. Proposed working model for 4-HNE-mediated Akt activation in hepatocytes. After exposure to 4-HNE, Akt is phosphorylated as a result of 4-HNE-mediated PTEN inhibition. This contributes to increased levels of lipid accumulation and cell survival.

(Lee et al., 2002; Leslie et al., 2003). The data presented in Figs. 6 and 8 verify, through the use of streptavidin purification of biotin hydrazide modified PTEN and MALDI-TOF MS, that PTEN is a novel target of 4-HNE within the cell and in vitro. In addition, PTEN lipid phosphatase assays presented in Fig. 5B demonstrate 4-HNE-mediated PTEN inhibition in HepG2 cells. Furthermore, as shown in Fig. 6, A and B, direct modification of recombinant PTEN by 4-HNE leads to inhibition of enzyme activity at low micromolar concentrations. Combined, these data provide a potential mechanism for Akt activation by 4-HNE. It should be stressed that these concentrations of 4-HNE are well within the physiological range in cells undergoing lipid peroxidation. Concentrations of 4-HNE within membranes have been calculated to be between 3.8 and 100 mM (Benedetti et al., 1984), and low micromolar concentrations of 4-HNE are known to occur during long-term sustained oxidative stress (Esterbauer et al., 1991; Tsukamoto et al., 1995).

The PTEN/Akt pathway is an important regulator of cell survival and fatty acid metabolism. Hepatospecific deletion of PTEN leads to increased steatosis via up-regulation of Akt (Horie et al., 2004). Deletion studies of both PTEN and Akt2, or Akt2 alone, demonstrated the necessity of the PTEN/Akt pathway in hepatic lipid accumulation (Leavens et al., 2009; He et al., 2010). Accumulation of liver triglycerides was significantly decreased in the PTEN(−/−)/Akt2(−/−) mice compared with PTEN(−/−) mice (He et al., 2010). This report demonstrates a significant increase, albeit modest, in lipid accumulation 24 h after 4-HNE addition to hepatocytes. Lipid accumulation could occur via Akt dependent biosynthetic pathways or it could be due to defects in lipid transport/β-oxidation. The activation of Akt by PTEN inhibition provides at least a partial mechanism for lipid increases exhibited after 4-HNE treatment.

4-HNE is an established biomarker for increased levels of oxidative stress in many chronic inflammatory diseases. Concentrations of 4-HNE within the cell have been estimated to be between 10 μM (cytosolic) and >3.8 mM (membrane) (Benedetti et al., 1984; Tsukamoto et al., 1995). PTEN is known to associate with membranes via its C2 domain placing it in an ideal position for interaction with 4-HNE (Lee et al., 1999). In this study, we find that treatment of HepG2 cells and primary rat hepatocytes with 4-HNE leads to increased Akt activation, as seen by increased phosphorylation at Ser473 and Thr308. Collectively, these experiments demonstrate a significant increase of 4-HNE-dependent fatty acid accumulation in HepG2 cells. The mechanism of Akt activation by 4-HNE is likely due to direct modification of PTEN by 4-HNE leading to inhibition of lipid phosphatase activity (Scheme 1). Akt activation during chronic inflammation in vivo may be due in part to 4-HNE-mediated PTEN inhibition, further contributing to increased steatosis in both nonalcoholic steatohepatitis and chronic ethanol models.

Authorship Contributions

Participated in research design: Shearn and Stewart.

Conducted experiments: Shearn, Stewart, and Fritz.

Contributed new reagents or analytic tools: Smathers and Hail.

Wrote or contributed to the writing of the manuscript: Shearn, Smathers, Stewart, Fritz, and Galligan.

Other: Petersen provided funding for the research.

References

Bayascas JR (2008) Dissecting the role of the 3-phosphoinositide-dependent protein kinase-1 (PDK1) signalling pathways. *Cell Cycle* **7:**2978–2982.

Benedetti A, Comporti M, Fulceri R, and Esterbauer H (1984) Cytotoxic aldehydes originating from the peroxidation of liver microsomal lipids. Identification of 4,5-dihydroxydecenal. *Biochim Biophys Acta* **792:**172–181.

Carbone DL, Doorn JA, Kiebler Z, and Petersen DR (2005) Cysteine modification by lipid peroxidation products inhibits protein disulfide isomerase. *Chem Res Toxicol* **18:**1324–1331.

Cho SH, Lee CH, Ahn Y, Kim H, Kim H, Ahn CY, Yang KS, and Lee SR (2004) Redox regulation of PTEN and protein tyrosine phosphatases in H(2)O(2) mediated cell signaling. *FEBS Lett* **560:**7–13.

Di Cristofano A and Pandolfi PP (2000) The multiple roles of PTEN in tumor suppression. *Cell* **100:**387–390.

Dozza B, Smith MA, Perry G, Tabaton M, and Strocchi P (2004) Regulation of glycogen synthase kinase-3beta by products of lipid peroxidation in human neuroblastoma cells. *J Neurochem* **89:**1224–1232.

Esterbauer H, Schaur RJ, and Zollner H (1991) Chemistry and biochemistry of 4-hydroxynonenal, malonaldehyde and related aldehydes. *Free Radic Biol Med* **11:**81–128.

Fang J and Holmgren A (2006) Inhibition of thioredoxin and thioredoxin reductase by 4-hydroxy-2-nonenal in vitro and in vivo. *J Am Chem Soc* **128:**1879–1885.

Go YM, Halvey PJ, Hansen JM, Reed M, Pohl J, and Jones DP (2007) Reactive aldehyde modification of thioredoxin-1 activates early steps of inflammation and cell adhesion. *Am J Pathol* **171:**1670–1681.

Grattagliano I, Caraceni P, Calamita G, Ferri D, Gargano I, Palasciano G, and Portincasa P (2008) Severe liver steatosis correlates with nitrosative and oxidative stress in rats. *Eur J Clin Invest* **38:**523–530.

Grimsrud PA, Picklo MJ Sr, Griffin TJ, and Bernlohr DA (2007) Carbonylation of adipose proteins in obesity and insulin resistance: identification of adipocyte fatty acid-binding protein as a cellular target of 4-hydroxynonenal. *Mol Cell Proteomics* **6:**624–637.

Hartley DP and Petersen DR (1997) Co-metabolism of ethanol, ethanol-derived acetaldehyde, and 4-hydroxynonenal in isolated rat hepatocytes. *Alcohol Clin Exp Res* **21:**298–304.

Hartley DP, Ruth JA, and Petersen DR (1995) The hepatocellular metabolism of 4-hydroxynonenal by alcohol dehydrogenase, aldehyde dehydrogenase, and glutathione S-transferase. *Arch Biochem Biophys* **316:**197–205.

He L, Hou X, Kanel G, Zeng N, Galicia V, Wang Y, Yang J, Wu H, Birnbaum MJ, and Stiles BL (2010) The critical role of AKT2 in hepatic steatosis induced by PTEN loss. *Am J Pathol* **176:**2302–2308.

Horie Y, Suzuki A, Kataoka E, Sasaki T, Hamada K, Sasaki J, Mizuno K, Hasegawa G, Kishimoto H, Iizuka M, et al. (2004) Hepatocyte-specific Pten deficiency results in steatohepatitis and hepatocellular carcinomas. *J Clin Invest* **113:**1774–1783.

Leavens KF, Easton RM, Shulman GI, Previs SF, and Birnbaum MJ (2009) Akt2 is required for hepatic lipid accumulation in models of insulin resistance. *Cell Metab* **10:**405–418.

Lee JO, Yang H, Georgescu MM, Di Cristofano A, Maehama T, Shi Y, Dixon JE, Pandolfi P, and Pavletich NP (1999) Crystal structure of the PTEN tumor suppressor: implications for its phosphoinositide phosphatase activity and membrane association. *Cell* **99:**323–334.

Lee SR, Yang KS, Kwon J, Lee C, Jeong W, and Rhee SG (2002) Reversible inactivation of the tumor suppressor PTEN by H2O2. *J Biol Chem* **277:**20336–20342.

Leslie NR, Bennett D, Lindsay YE, Stewart H, Gray A, and Downes CP (2003) Redox regulation of PI 3-kinase signalling via inactivation of PTEN. *EMBO J* **22:**5501–5510.

Liao Y and Hung MC (2010) Physiological regulation of Akt activity and stability. *Am J Transl Res* **2:**19–42.

Liu W, Akhand AA, Takeda K, Kawamoto Y, Itoigawa M, Kato M, Suzuki H, Ishikawa N, and Nakashima I (2003) Protein phosphatase 2A-linked and -unlinked caspase-dependent pathways for downregulation of Akt kinase triggered by 4-hydroxynonenal. *Cell Death Differ* **10:**772–781.

Marshall AJ, Krahn AK, Ma K, Duronio V, and Hou S (2002) TAPP1 and TAPP2 are targets of phosphatidylinositol 3-kinase signaling in B cells: sustained plasma membrane recruitment triggered by the B-cell antigen receptor. *Mol Cell Biol* **22:**5479–5491.

McMillian MK, Grant ER, Zhong Z, Parker JB, Li L, Zivin RA, Burczynski ME, and Johnson MD (2001) Nile Red binding to HepG2 cells: an improved assay for in vitro studies of hepatosteatosis. *In Vitr Mol Toxicol* **14:**177–190.

Ozeki M, Miyagawa-Hayashino A, Akatsuka S, Shirase T, Lee WH, Uchida K, and Toyokuni S (2005) Susceptibility of actin to modification by 4-hydroxy-2-nonenal. *J Chromatogr B Analyt Technol Biomed Life Sci* **827:**119–126.

Paradis V, Kollinger M, Fabre M, Holstege A, Poynard T, and Bedossa P (1997) In situ detection of lipid peroxidation by-products in chronic liver diseases. *Hepatology* **26:**135–142.

Poli G, Schaur RJ, Siems WG, and Leonarduzzi G (2008) 4-hydroxynonenal: a membrane lipid oxidation product of medicinal interest. *Med Res Rev* **28:**569–631.

Raza H and John A (2006) 4-hydroxynonenal induces mitochondrial oxidative stress, apoptosis and expression of glutathione S-transferase A4–4 and cytochrome P450 2E1 in PC12 cells. *Toxicol Appl Pharmacol* **216:**309–318.

Roede JR, Stewart BJ, and Petersen DR (2008) Decreased expression of peroxiredoxin 6 in a mouse model of ethanol consumption. *Free Radic Biol Med* **45:**1551–1558.

Seki S, Kitada T, Yamada T, Sakaguchi H, Nakatani K, and Wakasa K (2002) In situ detection of lipid peroxidation and oxidative DNA damage in non-alcoholic fatty liver diseases. *J Hepatol* **37:**56–62.

Shan X, Czar MJ, Bunnell SC, Liu P, Liu Y, Schwartzberg PL, and Wange RL (2000) Deficiency of PTEN in Jurkat T cells causes constitutive localization of Itk to the plasma membrane and hyperresponsiveness to CD3 stimulation. *Mol Cell Biol* **20:**6945–6957.

Sorrentino P, Terracciano L, D'Angelo S, Ferbo U, Bracigliano A, Tarantino L, Perrella A, Perrella O, De Chiara G, Panico L, et al. (2010) Oxidative stress and

steatosis are cofactors of liver injury in primary biliary cirrhosis. *J Gastroenterol* **45:**1053–1062.
Stewart BJ, Doorn JA, and Petersen DR (2007) Residue-specific adduction of tubulin by 4-hydroxynonenal and 4-oxononenal causes cross-linking and inhibits polymerization. *Chem Res Toxicol* **20:**1111–1119.
Stewart BJ, Roede JR, Doorn JA, and Petersen DR (2009) Lipid aldehyde-mediated cross-linking of apolipoprotein B-100 inhibits secretion from HepG2 cells. *Biochim Biophys Acta* **1791:**772–780.
Tjalkens RB, Cook LW, and Petersen DR (1999) Formation and export of the glutathione conjugate of 4-hydroxy-2, 3-E-nonenal (4-HNE) in hepatoma cells. *Arch Biochem Biophys* **361:**113–119.
Tsukamoto H, Horne W, Kamimura S, Niemelä O, Parkkila S, Ylä-Herttuala S, and Brittenham GM (1995) Experimental liver cirrhosis induced by alcohol and iron. *J Clin Invest* **96:**620–630.
Vazquez F, Grossman SR, Takahashi Y, Rokas MV, Nakamura N, and Sellers WR (2001) Phosphorylation of the PTEN tail acts as an inhibitory switch by preventing its recruitment into a protein complex. *J Biol Chem* **276:**48627–48630.
Watanabe S, Horie Y, and Suzuki A (2005) Hepatocyte-specific Pten-deficient mice as a novel model for nonalcoholic steatohepatitis and hepatocellular carcinoma. *Hepatol Res* **33:**161–166.
Wullschleger S, Wasserman DH, Gray A, Sakamoto K, and Alessi DR (2011) Role of TAPP1 and TAPP2 adaptors binding to PtdIns(3,4)P2 in regulating insulin sensitivity defined by knock-in analysis. *Biochem J* **434:**265–274.
Yu CX, Li S, and Whorton AR (2005) Redox regulation of PTEN by S-nitrosothiols. *Mol Pharmacol* **68:**847–854.

Address correspondence to: Dennis R. Petersen, 12850 East Montview Blvd., V20-2232C, Aurora, CO 80045. E-mail: dennis.petersen@ucdenver.edu